Integrative and Comparative Biology

Integrative and Comparative Biology, volume 00, number 0, pp. 1–14
https://doi.org/10.1093/icb/icac057

Society for Integrative and Comparative Biology

SYMPOSIUM

Kinematic Trajectories in Response to Speed Perturbations in Walking Suggest Modular Task-Level Control of Leg Angle and Length

M. J. Schwaner [*], K. C. Nishikawa [†‡] and M. A. Daley [*†,1]

[*]Department of Ecology and Evolutionary Biology, University of California, Irvine, Irvine, CA 92697, USA; [†]Center for Integrative Movement Sciences, University of California, Irvine, Irvine, CA 92697, USA; [‡]Department of Biology, Northern Arizona University, Flagstaff, AZ 86011, USA

From the symposium "Evolutionary conservation and diversity in a key vertebrate behavior: "walking" as a model system" presented at the annual meeting of the Society for Integrative and Comparative Biology virtual annual meeting, January 3–February 28, 2022.

[1]E-mail: madaley@uci.edu

Synopsis Navigating complex terrains requires dynamic interactions between the substrate, musculoskeletal, and sensorimotor systems. Current perturbation studies have mostly used visible terrain height perturbations, which do not allow us to distinguish among the neuromechanical contributions of feedforward control, feedback-mediated, and mechanical perturbation responses. Here, we use treadmill-belt speed perturbations to induce a targeted perturbation to foot speed only, and without terrain-induced changes in joint posture and leg loading at stance onset. Based on previous studies suggesting a proximo-distal gradient in neuromechanical control, we hypothesized that distal joints would exhibit larger changes in joint kinematics, compared to proximal joints. Additionally, we expected birds to use feedforward strategies to increase the intrinsic stability of gait. To test these hypotheses, seven adult guinea fowl were video recorded while walking on a motorized treadmill, during both steady and perturbed trials. Perturbations consisted of repeated exposures to a deceleration and acceleration of the treadmill-belt speed. Surprisingly, we found that joint angular trajectories and center of mass fluctuations remain very similar, despite substantial perturbation of foot velocity by the treadmill belt. Hip joint angular trajectories exhibit the largest changes, with the birds adopting a slightly more flexed position across all perturbed strides. Additionally, we observed increased stride duration across all strides, consistent with feedforward changes in the control strategy. The speed perturbations mainly influenced the timing of stance and swing, with the largest kinematic changes in the strides directly following a deceleration. Our findings do not support the general hypothesis of a proximo-distal gradient in joint control, as distal joint kinematics remain largely unchanged. Instead, we find that leg angular trajectory and the timing of stance and swing are most sensitive to this specific perturbation, and leg length actuation remains largely unchanged. Our results are consistent with modular task-level control of leg length and leg angle actuation, with different neuromechanical control and perturbation sensitivity in each actuation mode. Distal joints appear to be sensitive to changes in vertical loading but not foot fore-aft velocity. Future directions should include *in vivo* studies of muscle activation and force–length dynamics to provide more direct evidence of the sensorimotor control strategies for stability in response to belt-speed perturbations.

Introduction

Ground birds such as guinea fowl are a useful comparative animal model for investigating fundamental principles of locomotion because they are capable athletes that use walking and running gaits that are dynamically similar to human gaits (Gatesy and Biewener 1991; Rubenson et al. 2004; Watson et al. 2010; Müller et al. 2016; Daley 2018; Daley and Birn-Jeffery 2018; Gatesy 1999b). Striding bipedal locomotion involves alternating support on two hindlimbs, and typically

Advance Access publication May 24, 2022

includes two distinct gaits: walking at slower speeds and running at faster speeds (Alexander 1984, 1991, 1992, 2004). The dynamics of both walking and running can be modeled as a spring-loaded inverted pendulum, in which the body is represented as a point mass supported by a compressive compliant leg spring during stance (McGeer 1990a, 1990b; Alexander 1992; Lee and Farley 1998; Geyer et al. 2006). In walking, the leg is stiff relative to applied loads and the body follows an inverted-pendulum motion, with the body highest at mid-stance and a passive exchange between kinetic and gravitational potential energy (Farley and Ferris 1998; Lee and Farley 1998). In running, the body follows a bouncing motion, with the lowest point at mid-stance, kinetic, and gravitational potential energy fluctuating in-phase, and elastic energy cycling in the musculoskeletal structures of the leg (Cavagna 1975; Cavagna and Kaneko 1977; Alexander 1992; Farley et al. 1993; Farley and Gonzalez 1996; Lee and Farley 1998).

The motion of the body center of mass of the body (CoM) during walking and running gaits is coordinated through two specific modes of whole leg actuation (1) leg angular cycling, with leg retraction associated with forward progression during stance, and leg protraction in the swing phase to reposition the leg, and (2) telescoping leg length actuation (compression and extension of the leg length), which is associated with elastic energy cycling, particularly in the distal joints of the leg. As movement speed increases, animals typically increase step length by oscillating the leg through a greater angular excursion during stance (Farley et al. 1993; Farley and Gonzalez 1996). These two basic modes of leg movement: leg angular cycling and leg length actuation, represent "task level" functional variables for effective bipedal locomotion. The "virtual leg" is represented by a line connecting the CoM to the toe, to summarize the combined actuation effect across all joints. The virtual leg representation enables us to relate joint-level function to the task-level functional variables that enable effective weight support and mechanical energy fluctuation in locomotion (McMahon and Cheng 1990; Farley et al. 1993; Blum et al. 2010, 2011, 2014; Müller et al. 2016). Effective coordination of leg angular cycling and leg-spring loading is critical for both speed control and stability in uneven terrain (Farley et al. 1993; Daley 2018). However, it remains an ongoing question how the individual muscles and joints are coordinated to achieve effective control of these task-level functional variables in locomotion (Yen et al. 2009; Blum et al. 2014; Ting et al. 2015).

Perturbation studies have been used to investigate the mechanisms that enable muscle and joint coordination for task-level control of leg function (Ferris et al. 1999a, 1999b; Moritz and Farley 2004; Daley and Biewener 2006; Daley et al. 2006; Müller et al. 2010; Birn-Jeffery et al. 2014; Blum et al. 2014; Gordon et al. 2015; Voloshina and Ferris 2015). Studies using terrain height perturbations have revealed that telescoping leg actuation is highly sensitive to altered vertical loading and foot-substrate interactions that occur with altered timing of ground contact when navigating variations in terrain height (Daley and Biewener 2006; Daley et al. 2006; Birn-Jeffery and Daley 2012; Birn-Jeffery et al. 2014; Blum et al. 2014; Müller et al. 2016). Leg length actuation occurs mainly at the ankle and tarsometatarso-phalangeal (TMP) joints, associated with compliant, spring-mediated actuation at the distal joints. When guinea fowl run over potholes and obstacles, the largest and most rapid changes in joint mechanics and neuromuscular control occur in the distal ankle and TMP joints (Daley et al. 2007; Gordon et al. 2015). These changes occur through a combination of rapid intrinsic mechanical response and short-latency reflex feedback (Daley et al. 2007; Daley and Voloshina 2009; Daley and Biewener 2011; Gordon et al. 2015). In contrast, leg angular cycling exhibits mechanically robust feedforward control, which is adjusted over long timescales to change speed or navigate visible obstacles (Birn-Jeffery and Daley 2012; Blum et al. 2014). Leg angular cycling is actuated mainly at the hip and knee in guinea fowl (Gatesy 1999a, 1999b; Daley et al. 2007; Rubenson and Marsh 2009). These findings suggest a proximo-distal division of task-level control of the leg, with the proximal joints regulating speed and anticipatory changes in propulsion through feedforward control, and the distal joints exhibiting greater mechanical sensitivity and sensorimotor responsiveness to rapidly stabilize body mechanical energy in response to terrain perturbations (Daley et al. 2007; Gordon et al. 2015; Daley and Birn-Jeffery 2018).

In previous uneven terrain perturbation studies, variations in terrain height induced complex changes in leg posture, leg loading, and velocity. For example, in an obstacle or upward step, the ankle joint is more flexed and the effective leg length at contact is decreased (Daley and Biewener 2011; Birn-Jeffery and Daley 2012; Gordon et al. 2015, 2020). Upward steps also result in shorter aerial phases with earlier ground contact, reduced vertical velocity at contact, and shallower leg contact angle, resulting in altered leg loading. Together, these changes lead to different kinematics and muscle–tendon dynamics in an early stance. Due to the complex dynamics of the perturbation, it is difficult to determine the individual effects of each factor on the mechanics and control of the perturbation response. Visible terrain height changes also add further complexity because it is difficult to estimate the contribution of visual sensory input in mediating anticipatory changes in leg control.

Here, we investigate kinematic variability and strategies for stability in response to perturbations in treadmill-belt speed during walking. The belt-speed perturbation contrasts previous studies of varying terrain height in three important ways: (1) belt-speed perturbations are not readily visible based on terrain features, and therefore, anticipatory strategies for negotiating the perturbation are limited; (2) the belt-speed perturbations alter only the foot speed during stance, without a large change in joint posture and loading geometry at the time of foot contact; and (3) belt-speed perturbations are likely to influence leg angular speed more than leg length actuation, unlike terrain height perturbations. In uneven terrains, leg posture and muscle–tendon length in distal muscles at the onset of foot contact are the main factors in leg loading, muscle–tendon force, and changes in body mechanical energy during stance (Daley and Voloshina 2009; Blum et al. 2011).

The goal of the current study is to use treadmill-belt speed perturbations to induce a targeted perturbation to foot speed only, without mechanically induced changes in joint posture and leg loading at the onset of stance. If the proximo-distal gradient in joint neuromechanical control generally holds regardless of the perturbation type, we hypothesize that the distal joints will exhibit greater changes in joint kinematics in response to the belt-speed perturbations. An alternative hypothesis is that, if joint control is coordinated through task-level modules to regulate leg angular cycling and leg length actuation separately, the foot-speed perturbation might primarily influence leg cycling rate and proximal joint kinematics. Finally, based on the unpredictability in the perturbation, we expect birds to exhibit feedforward changes in control strategy and kinematics to increase the intrinsic stability of gait. Such changes could include longer stance duration and increased duty factor, slower leg retraction rate, and increased leg angular excursion during stance (Daley and Usherwood 2010; Daley and Birn-Jeffery 2018).

Methods

Animals

Seven adult guinea fowl (*Numida meleagris*) were used for this study (four females, three males, 1.83 ± 0.14 kg). Animals were habituated to handling and trained on the treadmill before data collection sessions. All procedures were licensed and approved by the University of California Institutional Animal Care and Use Committee (AUP 20–048). The kinematic data reported here were collected as part of a larger experiment that included recordings of *in vivo* muscle function and therefore the animals were euthanized at the end of the experiments by an injection of Euthasol (390 mg ml^{-1}, pentobarbital sodium) while under deep isoflurane anesthesia (5%) delivered by mask.

Data collection

During an experiment, we recorded between 4 and 12 trials per individual (each 30 s long), divided over 1–3 days (2–6 trials per day). Birds moved on a motorized treadmill (Woodway, Waukesha, WI, USA) while we recorded videos at 200 Hz (Phantom VRI VEO, Ametek, Vision Research Inc., Wayne, NJ, USA). We collected data for steady-state locomotion at a speed of 0.67 m s^{-1}, and one speed-perturbation protocol. This speed was selected to reflect a typical comfortable walking speed.

Treadmill-belt speed perturbations

Belt-speed-perturbations were created by decelerating and accelerating the treadmill belt, starting from the steady-state speed (0.67 m s^{-1}). We applied a randomized sequence of acceleration–deceleration perturbations, in which the treadmill repeatedly decelerated by ~0.25 m s^{-1}, to a speed of ~0.42 m s^{-1}, followed by acceleration back to the original steady-state speed (Fig. 1B). The treadmill was controlled through a serial-port connection with a laptop and script written in MATLAB (2021b; Mathworks, Woburn MA). There was no sound or other cue associated with treadmill-belt speed changes during the experiment. Each perturbation trial started with at least 7 s of steady-speed locomotion. During a 30-s trial, up to nine perturbations were presented to the bird. Due to differences in the timing of strides relative to belt acceleration, birds encountered the perturbations stochastically. Considering this variation in how individuals encountered perturbations across strides and trials, we quantified the magnitude of the perturbation based on the velocity of the bird's foot during stance. The foot is stationary relative to the belt during midstance, so the foot fore-aft horizontal speed during this time provides a good approximation of treadmill-belt speed. For each stride, we calculated the average velocity and acceleration of the foot during the period of 30–60% stance, which was determined from the steady-speed trials to be the time period when the foot is consistently stationary relative to the belt. We also estimated the average fore-aft foot/treadmill acceleration during this time to quantify the perturbation magnitude.

Data digitizing and processing

The kinematic analysis and stride categories were both based on the kinematics of the left leg, which faced

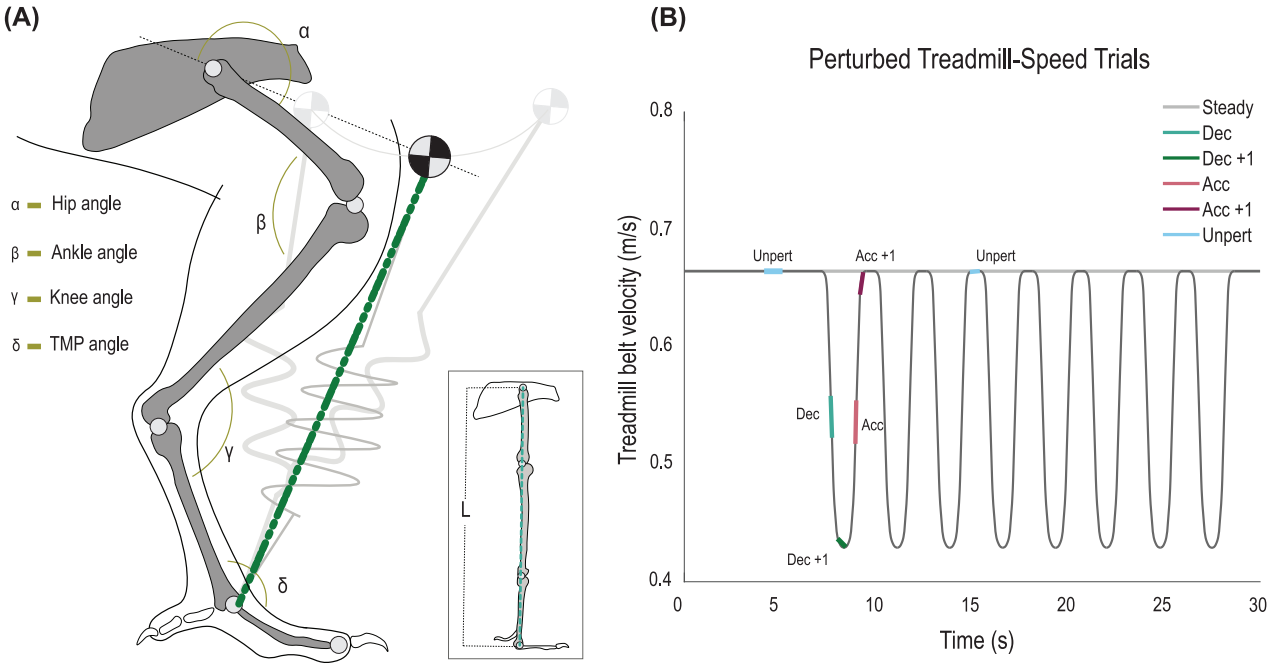

Fig. 1 (**A**) Schematic of a guinea fowl hind leg in normal and fully extended (inset) positions. We calculated joint angles for the hip, knee, ankle, and tarsometatarso-phalangeal (TMP) joints. The effective leg length and angle were calculated based on the line between the estimated CoM location and TMP joint (dark green line), expressed as a percentage of total segment leg length (light green line in inset), which is equal to the sum of all intrinsic limb segment lengths excluding the foot (after Rubenson and Marsh 2003). (**B**) Schematic of a treadmill-belt speed perturbation trial. Each perturbed trial started with a steady speed for at least 6 s. Perturbations consisted of deceleration followed by an acceleration back to the steady belt speed. Stride categories were assigned based on treadmill-belt acceleration encountered by the bird's foot. Colored line segments indicate a typical sequence of strides during a perturbation (see text for further details).

the camera. Approximate locations of limb joint centers of rotation were marked using a combination of permanent marker (black medium Sharpie, Newell-Rubbermaid Office, Oak Brook, IL) and non-toxic paint (Painters, Elmer's Products Inc, Westerville, OH). We used DeepLabCut (version 2.2.1) (Mathis et al. 2018; Nath et al. 2019) to digitize the joint centers of rotation and additional markers of interest: hip, knee, ankle, tarsometatarso-phalangeal (TMP) joint, and the tip of the middle toe, in addition to six body markers along the chest and back. To train DeepLabCut, we labeled ~40 frames taken from four videos, across the different data collection days for each animal. We used a ResNet-50 based neural network with default parameters for at least 1,000,000 training iterations. This network was used to analyze all videos from the same individual. Raw marker location data were filtered using a Butterworth filter with a cut-off frequency of 30 Hz.

To estimate the CoM location, we identified six body markers, with three points along the back and three points located ventrally along the sternum. We calculated the centroid position of the body markers and then, calculated the CoM location as the mid-point of the line connecting the tracked body centroid point and the hip position because the tracked body point was positioned relatively cranially. The hip angle was measured as the angle between the femur segment and a segment between the hip location and the estimated location of the CoM (Fig. 1A). Ankle angle was calculated based on the angle between the tibiotarsus and tarsometatarsus, and the TMP joint angle was calculated as the angle between the tarsometatarsus and foot segment. Knee joint location was calculated based on the intersection of femur and tibiotarsus segment lengths because skin movement makes the knee marker location inaccurate (Rubenson and Marsh 2009). Segment lengths were measured post-mortem for each animal.

Effective leg length and leg angle approximation

A line segment between the CoM location and the foot marker was used to approximate the effective length and angle of the "virtual leg" (Fig. 1A). Leg angle was calculated based on the angle of the virtual leg relative to the right hand horizontal. Effective leg length was normalized to a percentage of total available leg length, calculated as the sum of the intrinsic leg segments, excluding the foot: the femur, tibiotarsus, and tarsometatar-

sus (Fig. 1A). The average effective leg length during stance represents the overall leg posture (e.g., crouched versus extended) during locomotion, and the leg length fluctuations reflect the effective telescoping leg actuation across all limb joints. The leg angle represents the effective retraction and protraction oscillations of the leg through the stride cycle, which typically follows a consistent sinusoidal pattern (Blum et al. 2014). We also measured the fluctuations in vertical height of the CoM and the change in CoM velocity during stance. Change in CoM velocity was calculated based on the difference between the velocity of the CoM marker and the treadmill-belt speed.

Stride categories

Trials were selected for analysis based on the bird's ability to maintain a reasonably stationary location on the treadmill in the middle of the video field of view. Data for each trial were divided into strides starting and ending midswing, identified based on minima in ankle joint angles. Treadmill contact (foot touchdown and foot takeoff) timings were calculated based on the vertical and horizontal velocity of the digitized foot marker. The foot contact timings detected based on foot velocity were spot-checked against the video recordings.

To quantify the treadmill-belt speed perturbation experienced at the bird's foot, we created stride categories based on the measured fore-aft acceleration of the foot during stance. For each stride, we calculated the average velocity and acceleration of the foot during the period of 30–60% stance. To categorize strides, we first calculated the mean and standard deviation (SD) of foot velocity and acceleration across all recorded strides. Strides were then categorized as decelerating (Dec) if foot acceleration was <1 SD below zero, and as accelerating (Acc) if >1 SD above zero. The first stride following deceleration was categorized as Dec +1, and the first stride following an acceleration as Acc +1. All remaining strides collected during perturbed treadmill trials occurred at the steady state belt speed and were categorized as unperturbed (UnPert, see Fig. 1B). Strides from trials with a consistently steady belt speed were categorized as steady (S). The deceleration and re-acceleration of the treadmill belt during the trial created a typical perturbation sequence of Dec, Dec +1, Acc, Acc +1, UnPert, with the Dec +1 occurring at the trough in treadmill-belt speed (Fig. 1B). To account for the covariance of treadmill speed and acceleration associated with the perturbation, we included average foot velocity for each stride as a covariate in the linear mixed-effects model (see below). All analyses were performed in MATLAB .

Statistical analysis

Linear mixed-effects ANOVA was used to test for the effect of treadmill acceleration on limb and joint kinematics. **Model 1** included only the intercept and Individual as a random effect [$Y \sim 1 + (1|\text{ind})$], used as a reference model and null hypothesis, which was then compared to three alternative models: **Model 2** with stride category (StrideCat) as a categorical fixed effect [$Y \sim 1 + \text{StrideCat}*X + (1|\text{ind})$], **Model 3** with StrideCat as a categorical fixed effect and foot speed (FtSpeed) as a continuous covarying factor [$Y \sim 1 + \text{StrideCat}*X + \text{FtSpeed}*X + (1|\text{ind})$], and, finally, **Model 4** with per-individual speed effects among the random coefficients [$Y \sim 1 + \text{StrideCat}*X + \text{FtSpeed}*X + (\text{FtSpeed}|\text{ind})$]. Candidate models were compared based on AIC, total adjusted R-squared, and log-likelihood ratio tests, which supported the selection of Model 4 as the best fit. For each variable analyzed, we first calculated the ANOVA test statistics, and if the StrideCat effect was found to be statistically significant after False Discovery Rate correction, we then calculated 95% confidence intervals (CIs) for the difference between steady and perturbed stride categories, based on marginal means after accounting for the random effects. Thus, the pairwise differences represent the mean and 95% CI for effect of StrideCat after accounting for the covariance effect of foot speed both within and across individuals.

Results

Measurement of the perturbations

Birds experienced foot acceleration perturbations with an average magnitude of -0.24 ± 0.02 m s^{-2} during deceleration and $+0.23 \pm 0.02$ m s^{-2} during acceleration (mean ± 95% CI). Strides categorized as Dec +1 were characterized by the lowest mean foot velocity during stance, occurring near the trough of the belt-speed perturbation profiles (Fig. 2). Deceleration strides (Dec) and acceleration strides (Acc) showed mean foot velocities of similar magnitudes, whereas Acc +1 strides exhibited the highest mean foot velocity. In this experiment, the perturbation was encountered stochastically and therefore, the strides were categorized based on foot acceleration (Fig. 2B). Nonetheless, we do find a consistent distribution of stride categories across individuals (Table 1). We categorized a total of 2179 strides, of which 844 were steady-speed strides (recorded from steady treadmill trials) and 1334 were strides from belt-speed perturbation trials. We categorized 241 decelerations (Dec), 151 "Dec +1" strides, 187 accelerations (Acc), 172 "Acc +1" strides, and 583 unperturbed strides (Table 1).

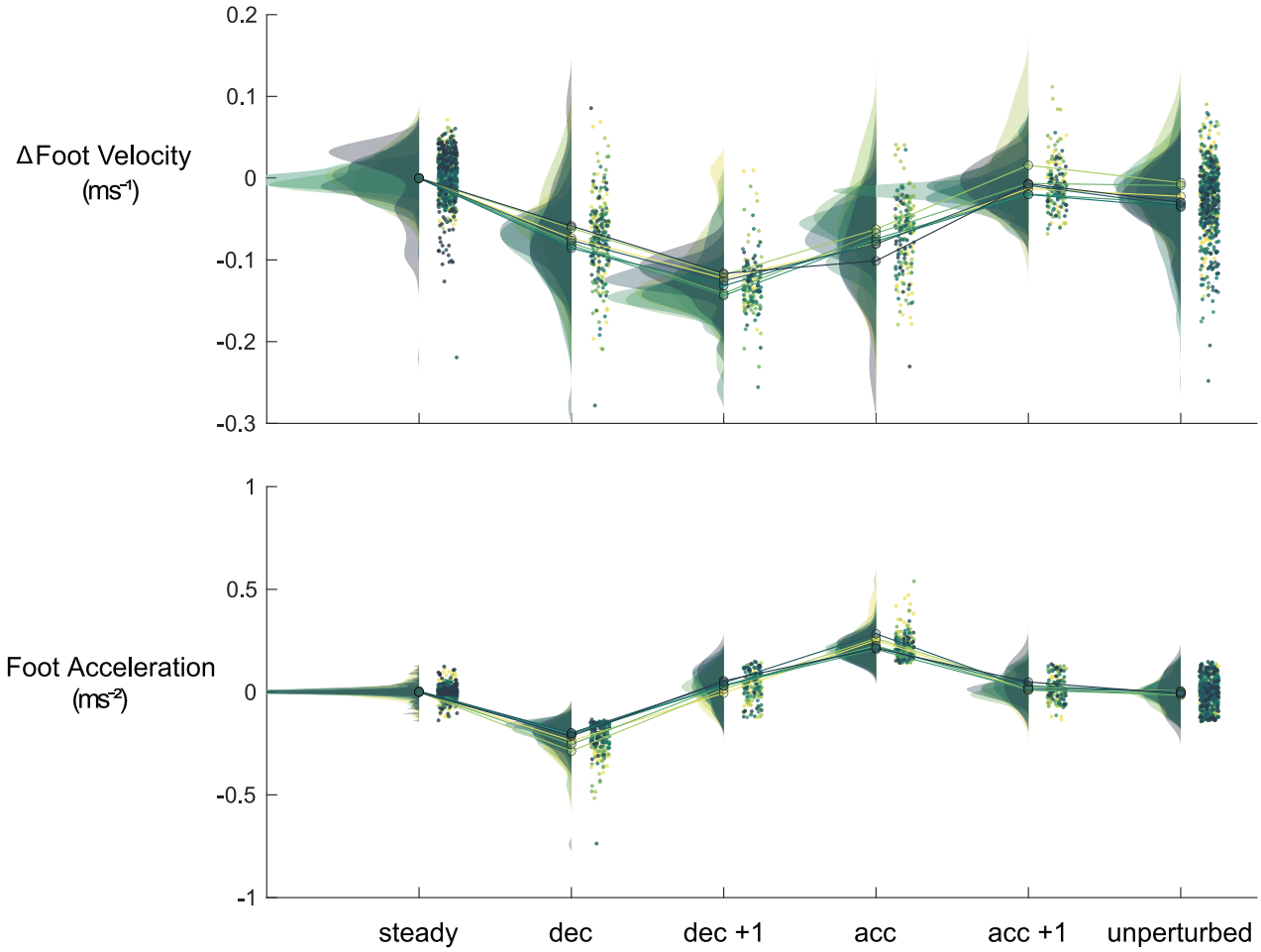

Fig. 2 Foot and treadmill fore-aft speed (top) and acceleration (bottom) during 30–60% stance across stride categories. Distributions and data points are shown in different colors for each individual. Lines connect stride categories for each individual, to help highlight individual variation in response.

Table 1 The sampling of stride categories across individuals

StrideCat	Ind1	Ind2	Ind5	Ind6	Ind7	Ind12	Ind13	Mean	St dev
Steady	124	119	126	104	121	140	111	121	11
Dec	50	36	46	20	37	39	13	34	13
Dec +1	25	24	29	15	22	30	6	22	8
Acc	46	27	38	17	24	25	10	27	12
Acc +1	39	24	34	19	20	26	10	25	10
Unperturbed	128	44	43	77	121	123	47	83	40

Strides per category are listed for each individual, with the mean and standard deviation for each stride category.

Changes in virtual leg kinematics and vertical oscillation of body CoM height

Despite the treadmill-belt speed perturbation, leg angle trajectories remained mostly within the 95% CI for steady-speed locomotion during stance, except Dec +1 strides (Fig. 2). The leg angular trajectory for Dec +1 deviates from the steady-speed immediately upon foot ground contact, with a lower rate of leg retraction, but following a similar sinusoidal pattern as other stride categories (Fig. 3). In perturbed strides, leg length was slightly lower on average throughout stance until the time of foot liftoff, compared to steady-speed trajectories. Although these trajectories are outside the 95% CI for steady-speed locomotion, the magnitudes of the deviations from steady speed are small. The vertical CoM height fluctuations show similar timing and magnitude across steady and perturbed strides, except for

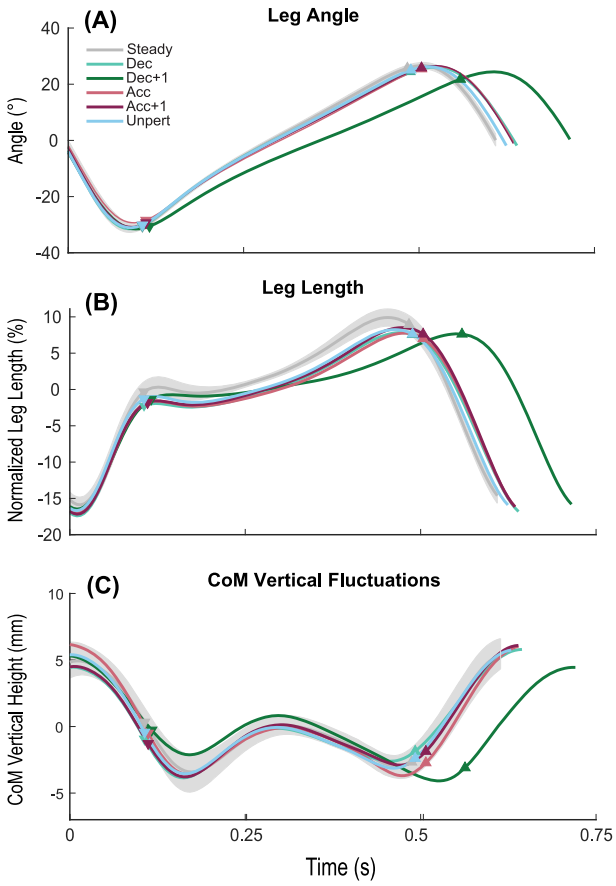

Fig. 3 Leg angle (**A**), leg length (**B**), and CoM vertical height trajectory (**C**) relative to the average value for steady locomotion. Gray lines and shading represent the 95% CI for steady strides at a constant treadmill speed. Colored lines show average trajectory for stride categories in the perturbation trials. Steady-state speed averages were subtracted from each trajectory, so that the trajectories oscillate around zero. Down-pointing triangles indicate foot touchdown, and upward pointing triangles correspond to foot takeoff. Vertical height trajectory (**C**) shows the highest variation across strides, relative to the typical magnitude of within stride fluctuations. Leg angular trajectory (**A**) exhibits low variance across strides, relative to within stride fluctuations.

the longer duration of the falling CoM phase in late stance in Dec +1, associated with the slowing of leg retraction and leg extension (Fig. 3). The magnitude of vertical displacement of CoM height was not significantly different in most perturbed strides, except for a slight increase in magnitude of CoM height excursion in Acc +1 strides. Overall, the changes in vertical CoM trajectory are small and mostly relate to changes in timing (see also Supplementary Fig. 1), suggesting consistent vertical loading across steady and perturbed strides.

Despite consistent overall trajectories and vertical CoM displacement, there were significant differences in kinematic timing in response to the perturbations. In Dec strides, the stride period increased significantly by 18 ± 14 ms (Fig. 4, Table 2). Stance duration was not significantly different from steady state, indicating that the change in timing occurs mainly in the swing period following the decelerated stance phase (Fig. 3). In Dec +1 strides, stance duration increased by 54 ± 19 ms, and stride duration increased by 81 ± 17 ms, indicating changes in both stance and swing periods. Despite these changes in stance and stride durations, the net angular excursion during stance remained relatively consistent, with a small decrease in Dec +1 strides (-3 ± 1 deg) and Acc strides (-2 ± 1 deg). This indicates that the magnitude of the oscillations in leg length and leg angle remained relatively consistent, although stance and stride timing changed considerably. The body CoM velocity relative to the foot decreases significantly in Dec +1 steps, by 0.29 ± 0.07 m s^{-1}, representing a ~43% decrease from the steady-state speed (Fig. 4), associated with the slowed rate of leg retraction and extension, particularly in late stance (Fig. 3). This suggests an active deceleration by the bird, separate from the direct effect of the belt-speed perturbation.

Changes in joint kinematics

Like the leg length and leg angle trajectories, the joint angular trajectories retained surprisingly consistent kinematics across steady and perturbed trials, with the perturbation in treadmill speed inducing relatively subtle changes (Fig. 5). The hip joint typically extended throughout stance, and exhibited lower rates of extension in perturbed strides, ending stance in a slightly more flexed position. This resulted in a small but significant decrease in net hip extension during stance in the perturbed strides (Fig. 6, Table 2). The Dec +1 strides, with an extended stance period, showed the greatest deviation in hip trajectory and net hip extension during stance. The knee joint typically flexed through most of stance, with a small and variable period of extension in late stance. In the perturbed strides, the knee trajectory remained nearly identical, except for the Dec +1 strides, in which flexion occurred more slowly over the prolonged stance duration, reaching a similar angle at the end of stance. There were no significant changes in net knee flexion during stance in the perturbed strides (Fig. 6, Table 2). The ankle joint typically flexed followed by extension during stance. In perturbed strides (Fig. 5), flexion magnitude was slightly reduced (Fig. 6, Table 2), suggesting an increase in stiffness, assuming similar loading. The TMP joint flexed continuously (dorsiflexion) through most of stance, with rapid extension (plantar-flexion) just before foot take-off. In perturbed trials, the flexion trajectory remained nearly identical but the timing of late-stance extension phase was delayed (Fig. 5). In Dec and Dec +1 strides, net joint

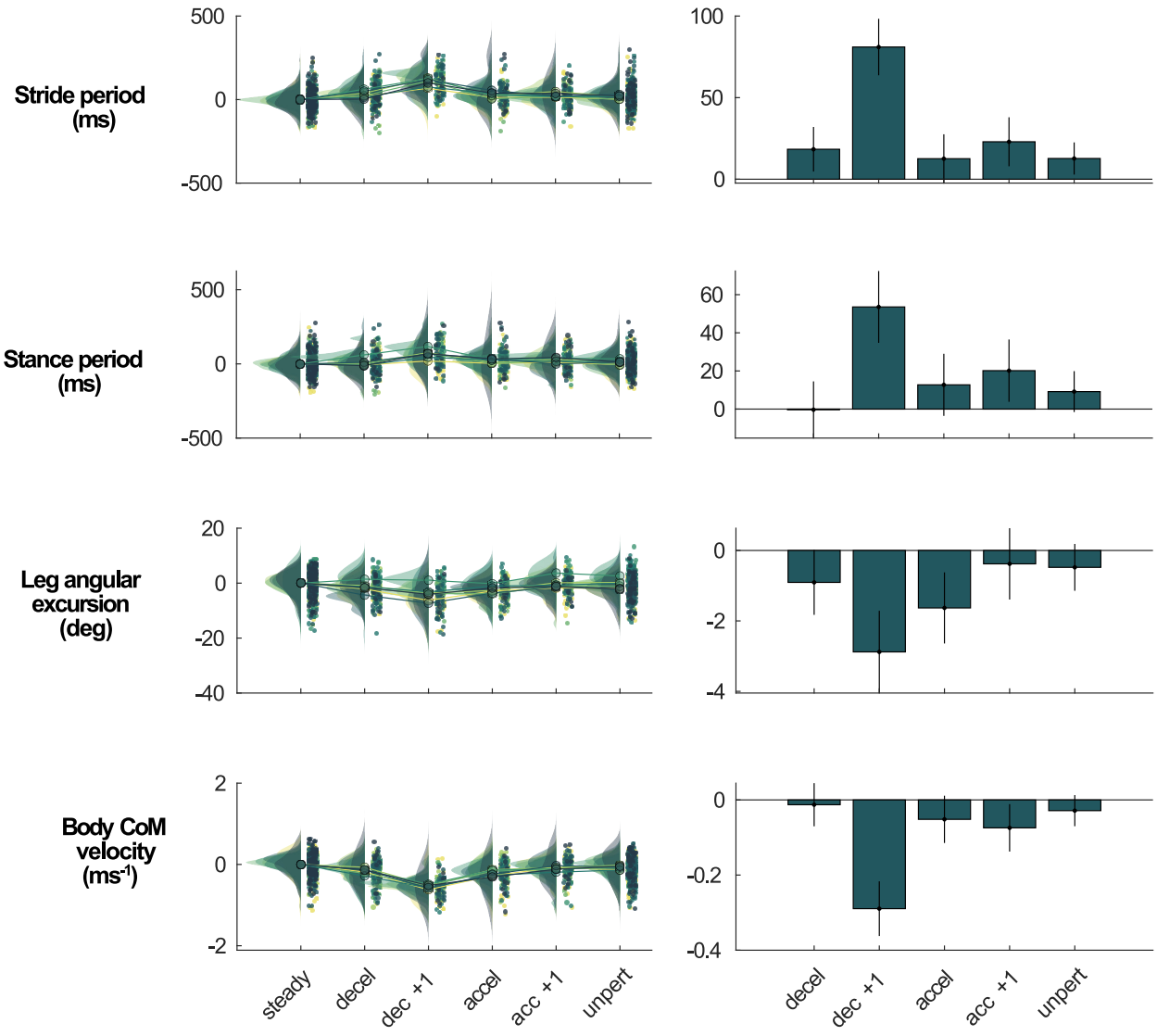

Fig. 4 Raincloud plot distributions and pairwise differences in perturbed stride categories compared to steady-speed walking for stride period, stance period, leg angular excursion, and change in body CoM velocity during stance (mean ± 95% CI).

extension decreased due to altered timing of foot take-off relative to TMP extension (Fig. 6, Table 2). Ankle and TMP joints exhibited consistent trajectories with a narrow 95% CI, demonstrating particularly low variance in the magnitude of joint angular fluctuations among individuals (Supplementary Fig. 2). The hip and knee joints exhibited slightly higher variance among individuals relative to the typical magnitude of joint angular changes.

Discussion

Here we showed that magnitudes of joint angle trajectories and CoM fluctuations remain remarkably consistent, despite a substantial perturbation of treadmill-belt speed. The proximal hip joint exhibits the greatest deviation in joint angular trajectory because the birds adopt a slightly more flexed position on average across all strides in the perturbed trials; nonetheless, changes in the hip net angular excursion during stance are small. The treadmill-belt speed perturbation mainly influenced timing of stance and swing, with the largest effect on the Dec +1 strides, after encountering belt deceleration. Our findings do not support the general hypothesis for a proximo-distal gradient in which distal joints always exhibit higher sensitivity to ground perturbations. Instead, the results support an alternative hypothesis for a functional, task-module based division of labor among joints for leg control, in which the hip joint actuates leg angular cycling for speed regulation and control of stance and swing phase timing, and the distal joints actuate leg length changes and responsiveness

Table 2 Linear mixed-effects ANOVA results with treadmill speed as a covariate (Model 4, see "Methods")

ANOVA F-stat			Stride category: pairwise difference from "Steady"				
Speed	**StrideCat**	**Variable name**	**Dec**	**Dec +1**	**Acc**	**Acc +1**	**Unperturbed**
7.30*	**8.03***	Δ Leg angle (deg)	−0.9 ± 0.9	**−2.9 ± 1.2***	**−1.6 ± 1.0***	−0.4 ± 1.0	−0.5 ± 0.7
0.93	**5.63***	Min LL (%)	−0.26 ± 1.18	1.24 ± 1.50	−0.48 ± 1.30	−0.83 ± 1.30	**−0.87 ± 0.85***
0.60	2.34	Δ Leg length (%)	0.36 ± 0.99	−0.73 ± 1.26	−0.36 ± 1.09	0.38 ± 1.09	−0.36 ± 0.72
0.31	**13.83***	LA_Fon (deg)	−0.1 ± 0.7	0.1 ± 0.9	**2.1 ± 0.8***	0.4 ± 0.8	0.4 ± 0.5
2.18	**7.19***	Hip ext (deg)	−1.0 ± 1.8	**−4.7 ± 2.3***	**−3.2 ± 2.0***	−0.9 ± 2.0	**−1.7 ± 1.3***
0.04	1.24	Knee flex (deg)	−0.4 ± 1.5	−1.2 ± 1.9	0.1 ± 1.6	−0.5 ± 1.6	−0.3 ± 1.1
0.97	**4.61***	Knee ext (deg)	**0.5 ± 0.4***	0.2 ± 0.5	−0.3 ± 0.4	−0.1 ± 0.4	0.0 ± 0.3
0.39	**27.51***	Ankle flex (deg)	**−1.5 ± 0.9***	**−3.9 ± 1.1***	**−3.4 ± 1.0***	**−2.1 ± 1.0***	**−1.6 ± 0.6***
4.71	**5.88***	Ankle ext (deg)	0.6 ± 1.0	**−2.0 ± 1.3***	0.2 ± 1.1	0.4 ± 1.1	0.2 ± 0.7
0.71	**8.77***	TMP flex (deg)	0.3 ± 1.6	0.6 ± 2.0	**−3.3 ± 1.8***	−0.1 ± 1.8	**−1.5 ± 1.2***
2.29	**10.75***	TMP ext (deg)	**−5.8 ± 3.5***	**−8.2 ± 4.5***	1.8 ± 3.9	0.8 ± 3.9	1.1 ± 2.5
13.80*	**28.20***	Stride period (ms)	**18.4 ± 13.7***	**81.0 ± 17.3***	12.6 ± 15.0	**23.0 ± 15.0***	**12.7 ± 9.9***
2.16	**13.28***	Stance period (ms)	−0.3 ± 14.9	**53.6 ± 18.8***	12.7 ± 16.3	**20.2 ± 16.3***	9.2 ± 10.7
66.95*	**22.44***	Δ CoM vel (m s^{-1})	−0.01 ± 0.06	**−0.29 ± 0.07***	−0.05 ± 0.06	**−0.07** ± 0.06*	−0.03 ± 0.04
0.06	**2.97***	Δ CoM height (mm)	1.2 ± 1.6	−0.2 ± 2.0	1.3 ± 1.7	**1.7 ± 1.7***	0.5 ± 1.1

Stride category was a fixed effect based on treadmill-belt acceleration during stance, with (FtSpeed | Individual)) as random effects. Degrees of freedom: speed = 1, StrideCat = 6, error = 2175. Asterisks indicate statistical significance.

to changes in ground-substrate interaction and vertical loading (Daley 2018). We found that the hip joint exhibits the largest changes in trajectory and timing in response to belt-speed perturbations, consistent with evidence that the hip regulates leg angular cycling for speed control. Additionally, stance and swing transitions retain consistent timing relative to hip angular trajectory (see Fig. 5). We found that the knee, ankle, and TMP joints exhibit nearly identical angular fluctuations during belt-speed perturbations, with the changes relating to timing in response to decelerated leg angular cycling and prolonged stance duration in the Dec +1 strides.

Interestingly, we found the largest changes in the kinematic timing of the recovery step following a deceleration, Dec +1. This suggests that the response to a perturbation of foot velocity is mediated through slower sensorimotor pathways, such as longer latency reflexes, central pattern generators or higher level control (Pearson 2000; Yakovenko et al. 2005; Frigon and Rossignol 2006). There is little change in vertical CoM height oscillation and distal joint trajectories in perturbed strides, suggesting consistent vertical leg loading. This might explain why there is little evidence of a rapid, reflex mediated response. Neurophysiological evidence suggests that leg angular cycling is regulated through feedforward control via central pattern generators, with position or velocity feedback at the hip regulating stance and swing transitions (Grillner and Rossignol 1978; Lam and Pearson 2002; McVea et al. 2005; Yakovenko et al. 2005; Frigon and Rossignol 2006). In contrast, distal joints are regulated through positive force feedback via short-latency reflexes, and exhibit rapid changes in activity in response to altered foot-substrate vertical loading (Andersson et al. 1978; Grillner and Rossignol 1978; Prochazka et al. 1997; Zehr and Stein 1999; Geyer et al. 2003; Donelan and Pearson 2004; Moritz and Farley 2004; Gordon et al. 2015). The current findings suggest that the rapid reflex-mediated responses observed in uneven terrain perturbations (Daley and Biewener 2011; Gordon et al. 2015, 2020) are not elicited in response to perturbations in foot velocity, at least under the conditions observed here. Instead, we observe a longer latency response that could reflect a behavioral change in response to the perception of the change in belt speed.

In addition to sensorimotor-mediated control, intrinsic mechanical control through multi-articular linkages is likely to be particularly important in the distal hindlimb of birds (Daley and Biewener 2006; Daley et al. 2006, 2007; Schaller et al. 2009; Backus et al. 2015; Daley 2018). Recently, the hypothesis for mechanical control of the distal limb was tested in a bird-inspired robot, BirdBot (Badri-Spröwitz et al. 2022). BirdBot uses elastically mediated actuation of the distal legs through a multi-articular tendon network, and achieves efficient walking and running with only two actuators in each leg, one at the hip and one at the knee. The hip actuator regulates leg angular cycling through a feedforward command, analogous to a central pattern generator. The knee actuator flexes the knee for the swing phase. Our current findings are consistent with the hypothesis of mechanically mediated control of the

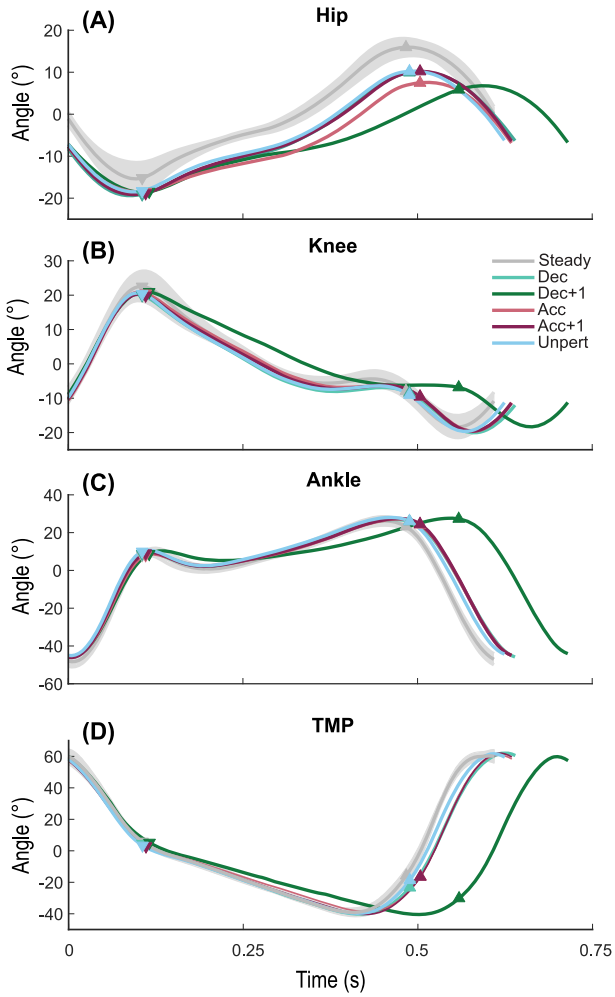

Fig. 5 Average joint angular trajectories for the hip (**A**), knee (**B**), ankle (**C**), and TMP (**D**). Mean joint angle for steady-speed strides has been subtracted from each trajectory before averaging. Light gray shading indicates a 95% CI across individuals for each stride category. Downward triangles indicate foot touchdown, whereas upward triangles indicate foot takeoff.

distal joints in the avian leg, with feedforward control of leg angular cycling at the hip to modulate speed and stance/swing transitions. The treadmill-belt perturbation altered foot speed but not vertical loading of the leg. We observed higher variance and greater changes in the hip joint trajectories, with an extension of the duration of leg retraction during stance (Figs. 5 and 6). Although the distal joints exhibited statistically significant differences in joint excursions during stance, the trajectories are nearly identical, and the changes occur primarily due to a change in the timing of late-stance extension relative to vertical foot velocity and take-off at the end of stance.

Previous perturbation studies used obstacles, potholes, and visible steps to investigate control mechanisms for stability. While these terrain perturbations are biologically relevant to navigation in real environments, they elicit complex changes in leg posture, vertical CoM velocity, and leg loading geometry (Daley and Biewener 2006; Daley et al. 2007; Birn-Jeffery and Daley 2012; Blum et al. 2014). Consequently, it is difficult to tease apart individual effects of postural, geometric, and muscle–tendon factors on the neuromechanics of the animals' response to the perturbation. Additionally, visible obstacle perturbations leave opportunity for visual contributions and anticipatory changes, making it difficult to parse out anticipatory versus reactionary responses. Here, the perturbations in treadmill-belt speed likely provide little visual signal, minimizing the opportunity for anticipatory strategies in the Dec strides, although the response to subsequent strides in the perturbation sequence likely includes changes in descending commands. We observe no evidence of rapid changes that would be consistent with short-latency reflexes in the kinematic trajectories. This could be in part due to the slow speed of the perturbation itself. We did see some evidence of feedforward changes in the hip angular trajectory because all strides in the perturbation trials show a slightly more flexed hip posture. These findings suggest some specific hypotheses for changes in neuromuscular control, which could be tested in future studies using *in vivo* measures of muscle activation, length, and force. In particular, we expect to find the largest changes in muscle recruitment in the Dec +1 stride, particularly at the hip, where we see substantial deceleration of hip angular trajectory. We additionally expect to find changes in recruitment and co-contraction of muscles at the ankle, because the decrease in ankle flexion suggests higher ankle stiffness, assuming similar vertical loads.

Virtual leg measurements, represented by a line segment connecting the CoM and the foot, summarize coordinated actuation of leg angle and leg length across all leg joints. With increasing gait speed, leg angular cycling rate increases, and legs undergo a larger angular excursion during stance (Farley et al. 1993; Farley and Gonzalez 1996). Coordination of leg angular cycling with leg-spring loading, has been identified as critical for maintaining speed and stability in uneven terrain navigation (Farley et al. 1993; Ferris et al. 1998, 1999a; Seyfarth et al. 2003; Daley and Biewener 2006; Blum et al. 2014; Daley 2018). Here, we found that CoM fluctuation magnitudes and trajectories are remarkably similar across strides in response to belt-speed perturbations. This suggests that the introduction of speed perturbations at the foot during walking does not influence CoM fluctuation magnitudes and vertical loading in guinea fowl. Additionally, we found that leg angular and leg length telescoping trajectories retain a very similar shape, with differences mainly in the timing. This is consistent with a strong influence of

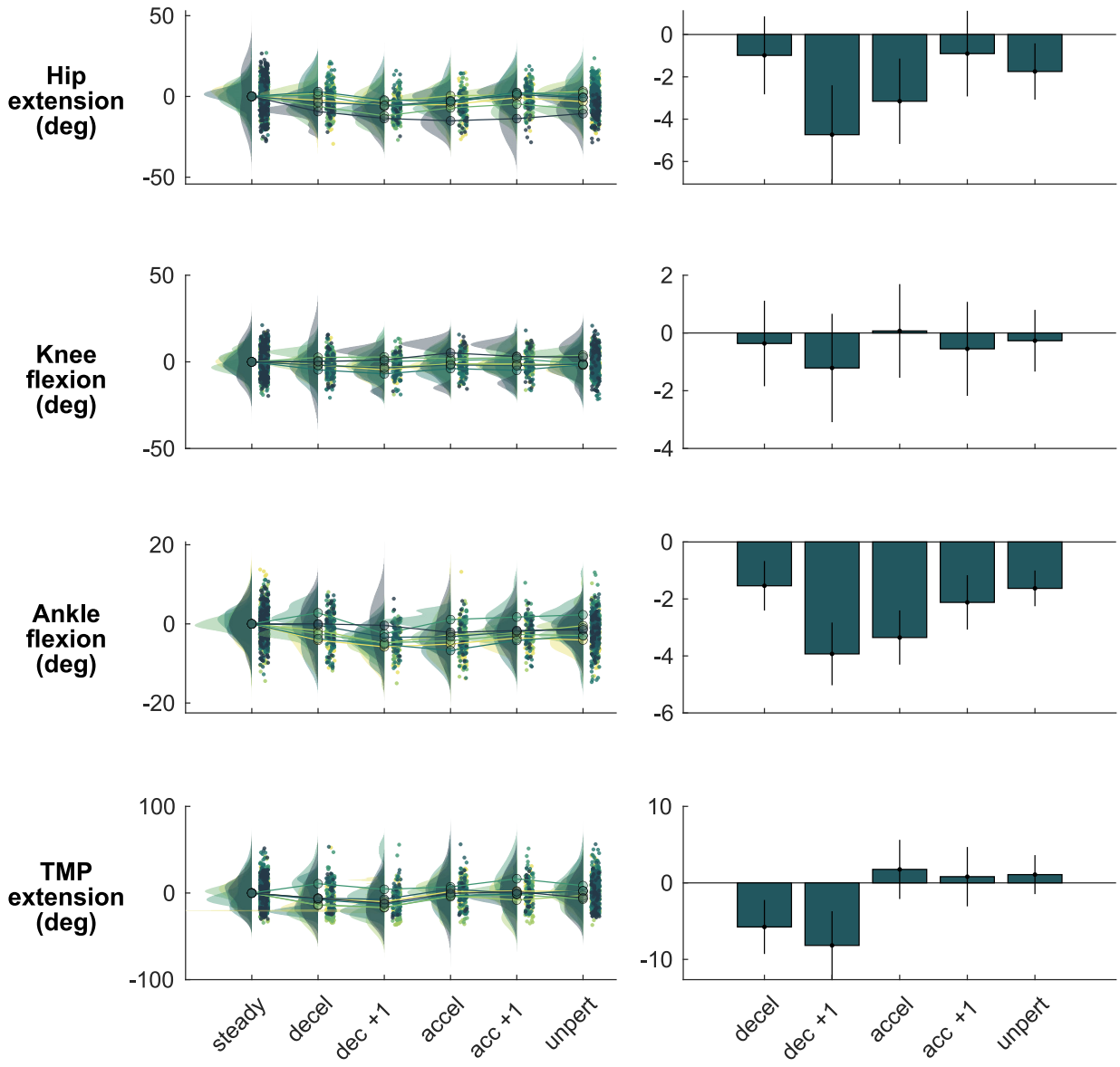

Fig. 6 Raincloud plot distributions and pairwise differences in perturbed stride categories compared to steady-speed walking for hip extension, knee flexion, ankle flexion, and TMP extension during stance (mean ± 5% CI).

feedforward central pattern generation in spinal networks. Stride period increased slightly across all strides in the perturbation trials, even unperturbed strides, suggesting a feedforward change in gait dynamics to increase stability in the perturbed conditions. Since speed is determined by the average belt speed, and speed is equal to stride length times stride frequency, longer stride period (lower stride frequency) is associated with longer stride lengths. Longer stride lengths increase the intrinsic mechanical stability of gait (Daley and Usherwood 2010; Daley and Birn-Jeffery 2018). However, the largest change in CoM velocity was observed in the Dec +1 stride, suggesting that the primary response to the perturbation was a longer latency behavioral response, likely involving the brain and descending pathways.

Sensorimotor control of muscles for terrestrial gait involves a combination of descending control based on current task and conditions, spinal central pattern generation, reflex-mediated feedback regulation and intrinsic mechanical control. Sensorimotor feedback response times are constrained by sensorimotor loop delays, with substantial delays associated with nerve conduction delay and excitation–contraction coupling inherent to the physiological properties of nerves and muscles (More et al. 2010; More and Donelan 2018). As the current perturbation impacts substrate/foot speed only, and is likely nearly invisible to the animal, we

expected no anticipatory within-stride responses, which is consistent with our findings. However, we are also surprised to see little evidence of reflex-mediated reactive responses to the speed perturbation. The consistent joint trajectories observed here suggest that the birds rely mainly on feedforward control of leg angular cycling, potentially with position-based feedback at the hip mediated swing/stance transitions. The findings are consistent with modular task-level control of leg angular cycling and leg length actuation (Auyang et al. 2009; McKay and Ting 2012; Ting et al. 2015), with different neuromechanical control of each task module. Vertical leg loading was not altered substantially by the speed perturbation; therefore, distal joint kinematics and leg length actuation remained largely unchanged. However, it is important to note that the current perturbation occurs over a longer period than the uneven terrain perturbations previously studied. Consequently, the differences may also relate to the different temporal characteristics of the perturbation itself.

Conclusions

Here, we showed that joint angle trajectories and CoM fluctuations remain remarkably similar in response to treadmill-belt speed perturbations at the foot. Perturbations mainly elicited changes in timing, especially during the first recovery stride after a deceleration. Belt-speed perturbations do not appear to elicit a rapid reflex-mediated response, based on kinematic trajectories. However, further investigation of muscle activity patterns is required to test whether or not there is a reflex-mediated change in stiffness at the ankle, or, instead, a feedforward increase in co-contraction across all strides in the perturbed trials. We see some suggestions of changes in feedforward control, through changes in hip angle and slight increases in stride duration across all strides in the perturbation trials. Our study is consistent with the hypothesis of modular task-level control of leg length and leg angular actuation, with different neuromechanical control of each task module. Our findings highlight the importance of considering specific mechanical effects of perturbations to predict and understand the likely mechanical and sensorimotor responses. Future studies of muscle activation and muscle force–length dynamics could shed further light on neuromechanical control mechanisms for stability in response to belt-speed perturbations and provide more insight into how animals navigate complex terrains.

Acknowledgments

This paper was part of the 2021 SICB symposium "Evolutionary conservation and diversity in a key vertebrate behavior: 'walking' as a model system." The authors would like to thank the organizers, Haley Amplo, Alice Gibb, and Sandy Kawano for their efforts. The authors would also like to thank Adrian Arias, Vivian Chong, Brooke Christensen, Catalina Dentzel, Kamila Karimjee, Zhiji Li, Elizabeth Mendoza, and Daisey Vega for help with data collection, and Chris Wagner for helping with the experimental set-up.

Funding

This work was supported by the National Science Foundation [grant number 2016049] to M.A.D. and K.C.N.

Supplementary data

Supplementary data available at *ICB* online.

Conflict of interest statement

The authors declare no conflict of interest.

Data availability statement

The data reported in this article are available through DataDryad at the following url: https://datadryad.org/stash/share/pRKlFEDwTZUmweqhbVpD08EmXt4swtEETzlJsF9MQEo.

References

Alexander RM. 1984. The gaits of bipedal and quadrupedal animals. Int J Rob Res 3: 49–59.

Alexander RM. 1991. Energy-saving mechanisms in walking and running. J Exp Biol 160: 55–69.

Alexander RM. 1992. A model of bipedal locomotion on compliant legs. Philos Trans R Soc Lond B Biol Sci 338: 189–98.

Alexander RM. 2004. Bipedal animals, and their differences from humans. J Anat 204: 321–30.

Andersson O, Grillner S, Lindquist M, Zomlefer M. 1978. Peripheral control of spinal pattern generators for locomotion in cat. Brain Res 150: 625–30.

Auyang AG, Yen JT, Chang Y-H. 2009. Neuromechanical stabilization of leg length and orientation through interjoint compensation during human hopping. Exp Brain Res 192: 253–64.

Backus SB, Sustaita D, Odhner LU, Dollar AM. 2015. Mechanical analysis of avian feet: multiarticular muscles in grasping and perching. R Soc Open Sci 2: 140350.

Badri-Spröwitz A, Aghamaleki Sarvestani A, Sitti M, Daley MA. 2022. BirdBot achieves energy-efficient gait with minimal control using avian-inspired leg clutching. Sci Robot 7: eabg4055.

Birn-Jeffery AV, Daley MA. 2012. Birds achieve high robustness in uneven terrain through active control of landing conditions. J Exp Biol 215: 2117–27.

Birn-Jeffery AV, Hubicki CM, Blum Y. 2014. Don't break a leg: running birds from quail to ostrich prioritise leg safety and economy on uneven terrain. J Exp Biol 217: 3786–97.

Blum Y, Birn-Jeffery A, Daley MA, Seyfarth A. 2011. Does a crouched leg posture enhance running stability and robustness? J Theor Biol 281: 97–106.
Blum Y, Lipfert SW, Rummel J, Seyfarth A. 2010. Swing leg control in human running. Bioinspir Biomim 5: 026006.
Blum Y, Vejdani HR, Birn-Jeffery AV, Hubicki CM, Hurst JW, Daley MA. 2014. Swing-leg trajectory of running guinea fowl suggests task-level priority of force regulation rather than disturbance rejection. PLoS One 9: e100399.
Cavagna GA, Kaneko M. 1977. Mechanical work and efficiency in level walking and running. J Physiol 268: 467–81.
Cavagna GA. 1975. Force platforms as ergometers. J Appl Physiol 39: 174–9.
Daley MA, Biewener AA. 2006. Running over rough terrain reveals limb control for intrinsic stability. Proc Natl Acad Sci U S A 103: 15681–6.
Daley MA, Biewener AA. 2011. Leg muscles that mediate stability: mechanics and control of two distal extensor muscles during obstacle negotiation in the guinea fowl. Philos Trans R Soc Lond B Biol Sci 366: 2693–707.
Daley MA, Birn-Jeffery A. 2018. Scaling of avian bipedal locomotion reveals independent effects of body mass and leg posture on gait. J Exp Biol 221: 153528.
Daley MA, Felix G, Biewener AA. 2007. Running stability is enhanced by a proximo-distal gradient in joint neuromechanical control. J Exp Biol 210: 383–94.
Daley MA, Usherwood JR, Felix G. 2006. Running over rough terrain: guinea fowl maintain dynamic stability despite a large unexpected change in substrate height. J Exp Biol 209: 171–87.
Daley MA, Usherwood JR. 2010. Two explanations for the compliant running paradox: reduced work of bouncing viscera and increased stability in uneven terrain. Biol Lett 6: 418–21.
Daley MA, Voloshina A. 2009. The role of intrinsic muscle mechanics in the neuromuscular control of stable running in the guinea fowl. J Physiol 587: 2693–707.
Daley MA. 2018. Understanding the agility of running birds: sensorimotor and mechanical factors in avian bipedal locomotion. Integr Comp Biol 58: 884–93.
Donelan JM, Pearson KG. 2004. Contribution of force feedback to ankle extensor activity in decerebrate walking cats. J Neurophysiol 92: 2093–104.
Farley CT, Ferris DP. 1998. Biomechanics of walking and running: center of mass movements to muscle action. Exerc Sport Sci Rev 28: 253–85.
Farley CT, Glasheen J, McMahon TA. 1993. Running springs: speed and animal size. J Exp Biol 185: 71–86.
Farley CT, Gonzalez O. 1996. Leg stiffness and stride frequency in human running. J Biomech 29: 181–6.
Ferris DP, Liang K, Farley CT. 1999a. Runners adjust leg stiffness for their first step on a new running surface. J Biomech 32: 787–94.
Ferris DP, Louie M, Farley CT. 1998. Running in the real world: adjusting leg stiffness for different surfaces. Proc R Soc Lond B Biol Sci 265: 989–94.
Frigon A, Rossignol S. 2006. Experiments and models of sensorimotor interactions during locomotion. Biol Cybern 95: 607–27.
Gatesy SM, Biewener AA. 1991. Bipedal locomotion: effects of speed, size and limb posture in birds and humans. J Zool 224: 127–47.
Gatesy SM. 1999a. Guineafowl hind limb function. II: Electromyographic analysis and motor pattern evolution. J Morphol 240: 127–42.
Gatesy SM. 1999b. Guineafowl hind limb function. I: Cineradiographic analysis and speed effects. J Morphol 240: 115–25.
Geyer H, Seyfarth A, Blickhan R. 2003. Positive force feedback in bouncing gaits? Proc R Soc Lond B Biol Sci 270: 2173–83.
Geyer H, Seyfarth A, Blickhan R. 2006. Compliant leg behaviour explains basic dynamics of walking and running. Proc R Soc Lond B Biol Sci 273: 2861–7.
Gordon JC, Holt NC, Biewener AA, Daley MA. 2020. Tuning of feedforward control enables stable muscle force-length dynamics after loss of autogenic proprioceptive feedback. Elife 9. e53908.
Gordon JC, Rankin JW, Daley MA. 2015. How do treadmill speed and terrain visibility influence neuromuscular control of guinea fowl locomotion?. J Exp Biol 218: 3010–22.
Grillner S, Rossignol S. 1978. On the initiation of the swing phase of locomotion in chronic spinal cats. Brain Res 146: 269–77.
Lam T, Pearson KG. 2002. The role of proprioceptive feedback in the regulation and adaptation of locomotor activity. In: Gandevia SC, Proske U, Stuart DG, editors. Sensorimotor control of movement and posture.Cham: Springer Nature. p. 343–55.
Lee CR, Farley CT. 1998. Determinants of the center of mass trajectory in human walking and running. J Exp Biol 201: 2935–44.
Mathis A, Mamidanna P, Cury KM, Abe T, Murthy VN, Mathis MW, Bethge M. 2018. DeepLabCut: markerless pose estimation of user-defined body parts with deep learning. Nat Neurosci 21: 1281–9.
McGeer T. 1990a. Passive bipedal running. Proc R Soc Lond B Biol Sci B240: 107–34.
McGeer T. 1990b. Passive dynamic walking. Int J Rob Res 9: 62–82.
McKay JL, Ting LH. 2012. Optimization of muscle activity for task-level goals predicts complex changes in limb forces across biomechanical contexts. PLoS Comput Biol 8: e1002465.
McMahon TA, Cheng GC. 1990. The mechanics of running: how does stiffness couple with speed? J Biomech 23: 65–78.
McVea DA, Donelan JM, Tachibana A, Pearson KG. 2005. A role for hip position in initiating the swing-to-stance transition in walking cats. J Neurophysiol 94: 3497–508.
More HL, Donelan JM. 2018. Scaling of sensorimotor delays in terrestrial mammals. Proc Biol Sci 285: 20180613.
More HL, Hutchinson JR, Collins DF, Weber DJ, Aung SKH, Donelan JM. 2010. Scaling of sensorimotor control in terrestrial mammals. Proc Biol Sci 277: 3563–8.
Moritz CT, Farley CT. 2004. Passive dynamics change leg mechanics for an unexpected surface during human hopping. J Appl Physiol 97: 1313–22.
Müller R, Birn-Jeffery AV, Blum Y. 2016. Human and avian running on uneven ground: a model-based comparison. J R Soc Interface 13: 20160529.
Müller R, Grimmer S, Blickhan R. 2010. Running on uneven ground: leg adjustments by muscle pre-activation control. Hum Mov Sci 29: 299–310.
Nath T, Mathis A, Chen AC, Patel A, Bethge M, Mathis MW. 2019. Using DeepLabCut for 3D markerless pose estimation across species and behaviors. Nat Protoc 14: 2152–76.

Pearson KG. 2000. Neural adaptation in the generation of rhythmic behavior. Annu Rev Physiol 62: 723–53.
Prochazka A, Gillard D, Bennett DJ. 1997. Positive force feedback control of muscles. J Neurophysiol 77: 3226–36.
Rubenson J, Heliams DB, Lloyd DG, Fournier PA. 2004. Gait selection in the ostrich: mechanical and metabolic characteristics of walking and running with and without an aerial phase. Proc Biol Sci 271: 1091–9.
Rubenson J, Marsh RL. 2003. Mechanical efficiency of limb swing during walking and running in guinea fowl (numida meleagris). J Appl Physiol 106: 1618–1630.
Rubenson J, Marsh RL. 2009. Mechanical efficiency of limb swing during walking and running in guinea fowl (Numida meleagris). J Appl Physiol 106: 1618–30.
Schaller NU, Herkner B, Villa R, Aerts P. 2009. The intertarsal joint of the ostrich (Struthio camelus): anatomical examination and function of passive structures in locomotion. J Anat 214: 830–47.
Seyfarth A, Geyer H, Herr H. 2003. Swing-leg retraction: a simple control model for stable running. J Exp Biol 206: 2547–55.
Ting LH, Chiel HJ, Trumbower RD, Allen JL, McKay JL, Hackney ME, Kesar TM. 2015. Neuromechanical principles underlying movement modularity and their implications for rehabilitation. Neuron 86: 38–54.
Voloshina AS, Ferris DP. 2015. Biomechanics and energetics of running on uneven terrain. J Exp Biol 218: 711–9.
Watson RR, Rubenson J, Coder L, Hoyt DF, Propert MWG, Marsh RL. 2010. Gait-specific energetics contributes to economical walking and running in emus and ostriches. Proc Biol Sci 278: 2040–6.
Yakovenko S, McCrea DA, Stecina K, Prochazka A. 2005. Control of locomotor cycle durations. J Neurophysiol 94: 1057–65.
Yen JT, Auyang AG, Chang Y-H. 2009. Joint-level kinetic redundancy is exploited to control limb-level forces during human hopping. Exp Brain Res 196: 439–51.
Zehr EP, Stein RB. 1999. What functions do reflexes serve during human locomotion? Prog Neurobiol 58: 185–205.